Analysis for Slip Flow Over a Single Free Disk With Heat Transfer

Aytac Arikoglu

Ibrahim Ozkol[1]

Faculty of Aeronautics and Astronautics, Istanbul Technical University, 34469 Maslak, Istanbul, Turkey

1 Introduction

In this study the equations of motion derived by von Karman [1], with Benton's transformations [2] for the flow over a single free disk is studied for the slip flow. The slip regime for the Knudsen number (Kn) is valid in the range $0.1 > Kn > 0.01$ [3]. For $Kn < 0.01$ the no-slip condition is present and for $Kn > 0.1$ the Navier–Stokes equations cannot be used since the flow field cannot be assumed to be continuum. In our study, the slip and the no-slip regimes that lie in the range $0.1 > Kn > 0$ is considered.

The subject of the rarefied gas dynamics can be conveniently defined as the study of gas flows in which the average value of the distance between two subsequent collisions of a molecule, namely the mean free path, is not negligible in comparison with a characteristic length of the structure considered. This type of flow is commonly encountered in many engineering aspects such as, high-altitude flight, micro-machines, vacuum technology, aerosol reactors, etc.

Mainly, requirement of high temperatures in the turbine stage of a gas turbine engine to achieve high thermal efficiencies, cooling of the air is essential to ensure for extending the life of turbine disks and blades. It is vital to know how flow and thermal fields are at every stage for a safe and effective work life, in the operation of the rotary type machine systems. For an accurate determination of temperature distribution, firstly the flow field must be solved as precisely as possible. Since the governing equations, namely the momentum equations, are highly nonlinear and coupled, it is hard to obtain exact analytical solutions for the full problem.

In 1921, von Karman [1] discovered the self similar behavior of the flow over a single free disk and solved the resulting ordinary differential equation system by using an approximate integral method. Latter, Cochran [4] obtained more accurate results by matching a Taylor series expansion near the disk with a series solution involving exponentially decaying functions far from the disk at a suitable mid point. Benton [2] improved Cochran's solutions and solved the problem for the unsteady case. The problem of heat transfer was first considered by Millsaps and Polhausen [5] for the values of Prandtl number (Pr) between 0.5 and 1.0. Then, Sparrow and Gregg [6] extended this work for a range of $0.1 < \mathrm{Pr} < 100$ by neglecting the dissipative terms in the energy equation.

In this study we used the differential transform method (DTM), which was introduced by Zhou [7] in a study about electrical circuits. It is semianalytical-numerical technique depending on Taylor series that is promising for various types of differential equations. With this technique, it is possible to obtain highly accurate results or exact solutions for the differential or integro-differential equation considered [8–10].

[1]Corresponding author. E-mail: ozkol@itu.edu.tr
Contributed by the Fluids Engineering Division for publication in the JOURNAL OF FLUIDS ENGINEERING. Manuscript received June 10, 2004; revised January 8, 2005. Associate Editor: Malcolm Andrews.

2 Theoretical Model for the Problem

Let (u,v,w) be the velocity components in the cylindrical coordinates (r,θ,z), respectively, and t be the temperature. Assuming that temperature is a function of the axial coordinate z only, the following similarity variables are introduced [1]:

$$u = \Omega r F(\zeta), \quad v = \Omega r G(\zeta), \quad w = \sqrt{\Omega \upsilon} H(\zeta),$$

$$p = -\rho \Omega \upsilon P(\zeta) \text{ and } T(\zeta) = (t - t_\infty)/(t_0 - t_\infty) \tag{1}$$

where, $\zeta = z\sqrt{\Omega/\nu}$ is the dimensionless axial coordinate. To solve the problem in a bounded domain, we use the following dependent and independent variables introduced by Benton [2]:

$$\xi = e^{-c\zeta} \tag{2}$$

$$F(\zeta) = c^2 f(\xi), \quad G(\zeta) = c^2 g(\xi), \quad H(\zeta) = -c[1 - h(\xi)] \tag{3}$$

Then, the Navier–Stokes equations and the energy equation, by neglecting dissipation terms, read:

$$\xi^2 f''(\xi) = f^2(\xi) - g^2(\xi) - \xi f'(\xi) h \tag{4}$$

$$\xi^2 g''(\xi) = 2f(\xi)g(\xi) - \xi g'(\xi) h(\xi) \tag{5}$$

$$\xi h'(\xi) = 2f(\xi) \tag{6}$$

$$T''(\zeta) = \mathrm{Pr} H T'(\zeta) \tag{7}$$

where, Pr is the Prandtl number. Since the assumption of continuum media fails, rarefied gases cannot be investigated with N.S. equations for a value of Knudsen number higher than 0.1 [11]. For the range $0.1 > Kn > 0.01$ the no slip B.C. cannot be used and should be replaced with the following expression [3]:

$$U_t = \frac{2-\sigma}{\sigma} \lambda \frac{\partial U_t}{\partial n} \tag{8}$$

where U_t is the tangent velocity, n is the normal direction to the wall, σ is the tangential momentum accommodation coefficient, and λ is the mean free path. For $Kn < 0.01$ the viscous flow is recovered and the no slip condition is valid. In our considerations the slip and the no-slip regimes of the Knudsen number that lies in the range $0.1 > Kn > 0$ will be taken into account. By using Eq. (8), the boundary conditions for the problem can be introduced as follows:

$$f(1) = \omega f'(1), \quad g(1) = c^{-2} - \omega c g'(1), \quad h(1) = 1 \tag{9}$$

$$f(0) = 0, \quad g(0) = 0, \quad h(0) = 0 \tag{10}$$

where, $\omega = [(2-\sigma)\lambda\Omega^{1/2}]/\sigma\nu^{1/2}$ is the slip factor. And the B.C.'s for the temperature are:

$$T(0) = 1, \quad T(\infty) = 0 \tag{11}$$

By integrating Eq. (7) with the first boundary condition in Eq. (11), the dimensionless temperature can be evaluated in terms of the axial part of the velocity field as follows:

$$T(\zeta) = T'(0) \int_0^{\zeta} e^{\mathrm{Pr}\int_0^{\beta} H(\eta) d\eta} d\beta + 1 \tag{12}$$

where, β and η are dummy variables. The missing B.C. $T'(0)$ is obtained from the far field B.C. given in Eq. (11) as follows:

$$T'(0) = -1 \Bigg/ \int_0^{\infty} e^{\mathrm{Pr}\int_0^{\beta} H(\eta) d\eta} d\beta \tag{13}$$

3 The Solution

In solving Eqs. (4)–(6) with the B.C.'s (9) and (10), we applied DTM at $\xi = 0$. By using the theorems in [8], the differential transform of Eqs. (4)–(6) can be evaluated as follows:

$$\widetilde{F}(k)=\frac{1}{k(k-1)}\sum_{l=0}^{k}\left[\widetilde{F}(l)\widetilde{F}(k-l)-\widetilde{G}(l)\widetilde{G}(k-l)-l\widetilde{F}(l)\widetilde{H}(k-l)\right] \tag{14}$$

$$\widetilde{G}(k)=\frac{1}{k(k-1)}\sum_{l=0}^{k}\left[2\widetilde{F}(l)\widetilde{G}(k-l)-l\widetilde{G}(l)\widetilde{H}(k-l)\right] \tag{15}$$

$$\widetilde{H}(k)=\frac{2}{k}\widetilde{F}(k) \tag{16}$$

where, $k\geqslant 2$ and $\widetilde{F}(k)$, $\widetilde{G}(k)$, and $\widetilde{H}(k)$ denote to the differential transforms of $f(\xi)$, $g(\xi)$, and $h(\xi)$, respectively. To evaluate the dependent variables, we need to know the missing B.C.'s $f'(0)$ and $g'(0)$. In many studies, such as [12], the shooting method is used to determine unknown B.C.'s. Instead of using the shooting method, we obtained the values of $\widetilde{F}(k)$, $\widetilde{G}(k)$ and $\widetilde{H}(k)$ for $k=2,3,\ldots,N$ in terms of $f'(0)$ and $g'(0)$, which will be called as f_1 and g_1 respectively, then by using the B.C.'s given in Eq. (9) for $\xi=1$, we evaluated f_1, g_1, and c numerically. This is much faster and cost efficient than the numerical techniques since it is not iterative. With the new defined ones, the B.C.'s given in Eq. (10) for $\xi=0$ are transformed as follows:

$$\widetilde{F}(0)=0,\quad \widetilde{G}(0)=0,\quad \widetilde{H}(0)=0,\quad \widetilde{F}(1)=f_1 \text{ and } \widetilde{G}(1)=g_1 \tag{17}$$

By using the recurrence relations in Eqs. (14)–(16) and the transformed boundary conditions in Eq. (17), $\widetilde{F}(k)$, $\widetilde{G}(k)$, and $\widetilde{H}(k)$ for $k=2,3,\ldots,N$ are evaluated. Then, using the inverse transformation rule in [8], the series solutions are obtained from:

$$f(\xi)=\sum_{k=0}^{N}\widetilde{F}(k)\xi^k,\quad g(\xi)=\sum_{k=0}^{N}\widetilde{G}(k)\xi^k,\quad h(\xi)\sum_{k=0}^{N}\widetilde{H}(k)\xi^k \tag{18}$$

where, N is the number of terms to be calculated. By calculating up to $N=6$, we get:

$$f(\xi)=f_1\xi-\tfrac{1}{2}(f_1^2+g_1^2)\xi^2+\tfrac{1}{4}f_1(f_1^2+g_1^2)\xi^3-\tfrac{1}{144}(17f_1^4+18f_1^2g_1^2 + g_1^4)\xi^4+\tfrac{1}{1152}f_1(61f_1^4+74f_1^2g_1^2+13g_1^4)\xi^5-\tfrac{1}{86400}(1971f_1^6 + 2825f_1^4g_1^2+889f_1^2g_1^4+35g_1^6)\xi^6+\cdots \tag{19}$$

$$g(\xi)=g_1\xi-\tfrac{1}{12}g_1(f_1^2+g_1^2)\xi^3+\tfrac{1}{18}f_1g_1(f_1^2+g_1^2)\xi^4-\tfrac{1}{1920}g_1(53f_1^4 + 58f_1^2g_1^2+5g_1^4)\xi^5+\tfrac{1}{5400}f_1g_1(65f_1^4+82f_1^2g_1^2+17g_1^4)\xi^6+\cdots \tag{20}$$

$$h(\xi)=2f_1\xi-\tfrac{1}{2}(f_1^2+g_1^2)\xi^2+\tfrac{1}{6}f_1(f_1^2+g_1^2)\xi^3-\tfrac{1}{288}(17f_1^4+18f_1^2g_1^2 + g_1^4)\xi^4+\tfrac{1}{2880}f_1(61f_1^4+74f_1^2g_1^2+13g_1^4)\xi^5-\tfrac{1}{259200}(1971f_1^6 + 2825f_1^4g_1^2+889f_1^2g_1^4+35g_1^6)\xi^6+\ldots \tag{21}$$

Table 2 Variation of $T'(0)$, f_1 and g_1 with respect to ω (N=60)

ω	$T'(0)$	f_1	g_1
0.0	−0.32586039	1.182244779	1.536776526
0.1	−0.333496950	1.096913972	1.422174786
0.2	−0.336780900	1.038943086	1.339504645
0.5	−0.334652873	0.942790947	1.191324451
1.0	−0.320432993	0.875499819	1.076800290
2.0	−0.292997980	0.825074692	0.983003210
5.0	−0.244046155	0.783417800	0.898674732
10.0	−0.205049245	0.765039980	0.858998126
20.0	−0.168829630	0.753582150	0.833355187

The solutions are given here up to $O(\xi^6)$, however, one can easily obtain higher ordered terms. After evaluating $f(\xi)$, $g(\xi)$, and $h(\xi)$, the original dependant variables $F(\zeta)$, $G(\zeta)$, and $H(\zeta)$ are obtained by using Eqs. (2) and (3). If necessary, $P(\zeta)$ can be obtained from the following equation:

$$P(\zeta)-P_0=H(\zeta)^2/2-H'(\zeta) \tag{22}$$

4 Results and Discussion

The variation of the flow field parameters $F'(0)$, $G'(0)$, and $H(\infty)=-c$ with respect to the slip factor are given below in Table 1 with comparison to [13]. The other parameters, which are f_1, g_1, and $T'(0)$ are reported in Table 2.

We evaluated the results in Tables 1 and 2 and Figs. 1–10 by calculating $N=60$ terms. One can see from Table 1 that the results obtained for $F'(0)$, $G'(0)$, and $H(\infty)$ are in good agreement with [13]. While evaluating the thermal field, we took Pr=0.71, which is the value of Prandtl number for air. By continuing the same procedure, the thermal field can be computed for other Prandtl numbers.

Figures 1 and 2 show that the magnitudes of the surface skin friction in radial and circumferential directions decrease with an increase in ω. This is quite natural since ω, the slip factor, is the ratio of slip to viscous effects. As a consequence and as it can be observed from Fig. 4, the inflow rate at infinity decreases since the radially outwards boundary layer loses its thickness and is fed by the fluid stream in axial direction.

As one can see from Fig. 3, the minimum value for $T'(0)$ is not reached at $\omega=0$. We calculated this value as $\omega=0.2836$ and the value corresponding to this point as $T'(0)=-0.337462$. This value of the slip factor is of great importance since the heat transfer from the rotating disk is directly related to the temperature gradient at $\zeta=0$. We can state that the maximum cooling of the rotating disk is reached at this value of the slip factor if the ambient fluid is colder than the rotating disk. The magnitudes of the radial and the circumferential velocities just above the rotating disk are given below in Figs. 5 and 6.

The highest value of the radial velocity on the surface is 0.128440 and this value is reached at $\omega=1.1586$. This value of the

Table 1 Variation of the flow field parameters due to ω with comparison to Ref. [13] (N=60)

ω	$F'(0)$	$F'(0)$ [13]	$G'(0)$	$G'(0)$ [13]	$H(\infty)$	$H(\infty)$ [13]
0.0	0.510232619	0.51023262	−0.615922014	−0.61592201	0.88447411	0.8844742
0.1	0.421453639	0.42145364	−0.605835241	−0.60583524	0.88136423	0.8813642
0.2	0.352581007	0.35258101	−0.583676764	−0.58367676	0.87395729	0.8739572
0.5	0.223848209	0.22384821	−0.502809702	−0.50280970	0.84239263	0.8423926
1.0	0.127923645	0.12792364	−0.394927595	−0.39492760	0.78947720	0.7894772
2.0	0.061010098	0.06101010	−0.273370132	−0.27337013	0.71031331	0.7103134
5.0	0.018588527	0.01858853	−0.143388209	−0.14338821	0.58376463	0.5837646
10.0	0.006812558	0.00681256	−0.081030089	−0.08103009	0.48758465	0.4875846
20.0	0.002361594	0.00236159	−0.043788462	−0.04378846	0.39997581	0.3999758

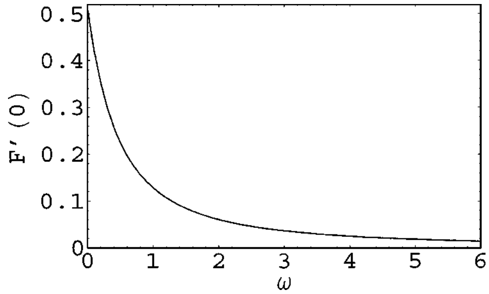

Fig. 1 Variation of $F'(0)$ with ω

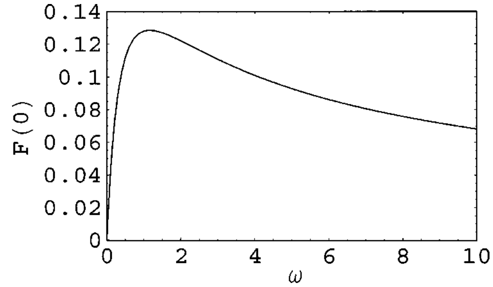

Fig. 5 Variation of the radial velocity with respect to ω at $\zeta=0$

slip factor may be necessary and important practically, if the aim is to use the disk as a centrifugal fan. As one can see from Fig. 6, the maximum circumferential velocity on the surface is at $\omega=0$, where the no-slip condition is present. This is a result of the negative gradient of the circumferential velocity in z direction above the disk. Variations of F, G, H, and T for several values of ω are given below in Figs. 7–10.

From Figs. 7–9, the decreasing effect of the slip factor ω on velocity field can be easily seen. In the limit case $\omega\to\infty$, when the flow is entirely potential, the rotating disk has no effect on rotating the fluid particles, therefore, the velocity field is constant and equal to zero.

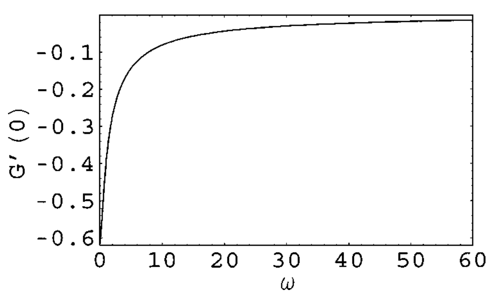

Fig. 2 Variation of $G'(0)$ with ω

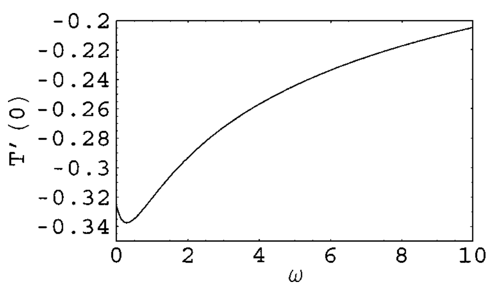

Fig. 3 Variation of $T'(0)$ with ω

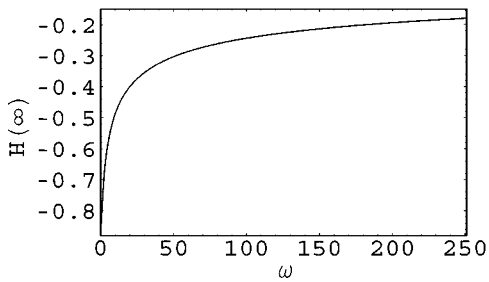

Fig. 4 Variation of $H(\infty)$ with ω

This is natural, since the rotating disk acts like a centrifugal fan and owing to the centrifugal forces, throws the fluid that sticks on it. A fluid stream compensates this thrown fluid, which is in the axial direction. When ω increases, less amount of fluid can stick and the rotating disk loses its efficiency to transfer its circumferential momentum to the fluid particles. The fluid loses circumferential velocity therefore the centrifugal forces that throw the fluid outwards decrease. Since the disk throws less fluid away, less amount of fluid stream in the axial direction exists.

From Fig. 10, one can conclude that as the slip factor ω increases, $T(\zeta)$ tends to vary linearly. This is a result of the fact that as ω increases, $H(\zeta)$ decrease and in the limit case of $\omega\to\infty$, $H=0$ can be taken. From Eq. (7), this leads to the following case:

$$\lim_{\omega\to\infty} T''(\zeta)=0 \tag{23}$$

where, the solution is a line and for large values of ω, it can be approximately taken as: $T(\zeta)\cong T'(0)\zeta+1$ to ease the computations, if necessary.

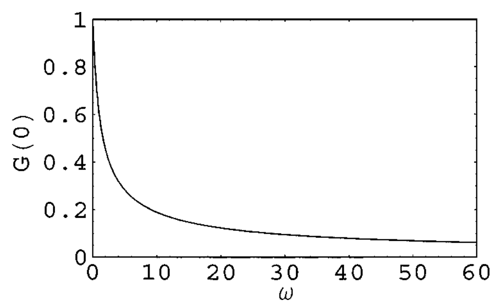

Fig. 6 Variation of circumferential velocity with respect to ω at $\zeta=0$

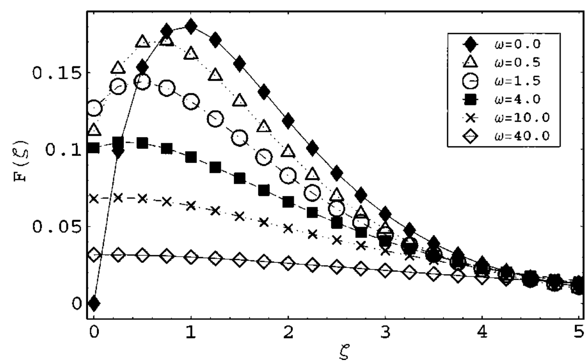

Fig. 7 Radial component of the velocity for several values of ω

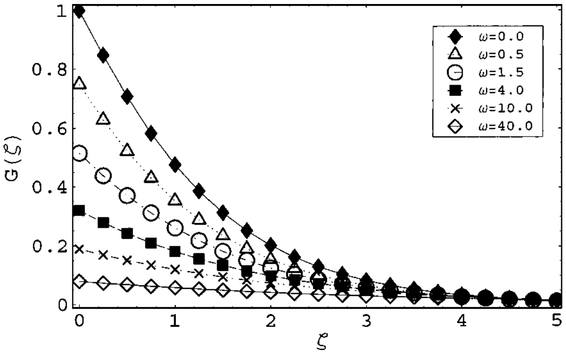

Fig. 8 Circumferential component of the velocity for several values of ω

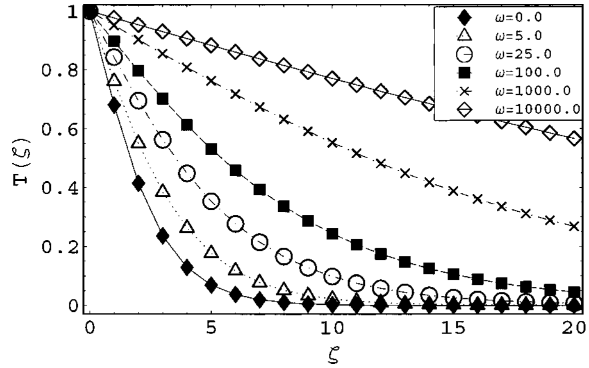

Fig. 10 Variation of temperature for several values of ω, Pr =0.71

5 Conclusion

In this study, the slip flow over a rotating infinite disk is considered. DTM is used as the solution technique after the domain is transformed to a bounded one. Velocity and thermal fields are evaluated accurately. Numerical and graphical results are given and the effect of slip to the flow field variables is discussed in detail. The point that is worth noticing in this paper is that robustness of the DTM since it solves nonlinear-coupled equations in a simplified and tractable manner with high accuracy. This study also diverges from the similar studies in literature by solving temperature field for the slip flow over a rotating disk.

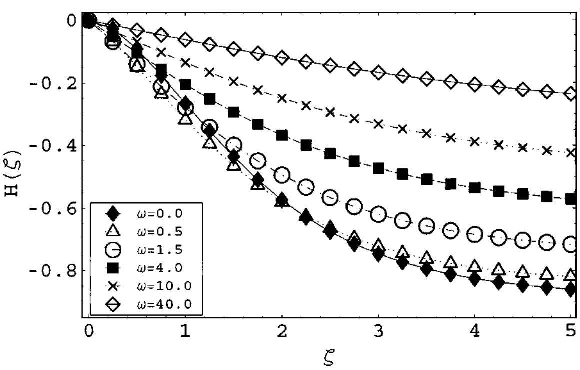

Fig. 9 Axial component of the velocity for several values of ω

References

[1] Karman, T., 1921, “Über Laminare und Turbulente Reibung,” Z. Angew. Math. Mech., **1**, pp. 233–252.

[2] Benton, E. R., 1966, “On the flow due to a rotating disc,” J. Fluid Mech., **24**, pp. 781–800.

[3] Sharipov, F. and Seleznev, V., 1998, “Data on internal rarefied gas flows,” J. Phys. Chem. Ref. Data, **27**, pp. 657–706.

[4] Cochran, W. G., 1934, “The flow due to a rotating disc,” Proc. Cambridge Philos. Soc., **30**, pp. 365–375.

[5] Millsaps, K., and Polhhausen, K., 1952, “Heat transfer by laminar flow from a rotating plate,” J. Aeronaut. Sci., **19**, pp. 120–126.

[6] Sparrow, E. M., and Gregg, J. L., 1959, “Heat transfer form a rotating disk to fluids of any Prandtl number,” ASME J. Heat Transfer, **81**, pp. 249–251.

[7] Zhou, J. K., 1986, *Differential Transformation and its Application for Electrical Circuits*, Huazhong University Press, Wuhan, China.

[8] Arikoglu, A. and Ozkol, I., 2004, “Solution of boundary value problems for integro-differential equations by using Differential Transform Method,” Appl. Math. Comput. (to be published).

[9] Ayaz, F., 2003, “On the two-dimensional differential transform method,” Appl. Math. Comput., **143**, pp. 361–374.

[10] Ayaz. F., 2004, “Solutions of the system of differential equations by differential transform method,” Appl. Math. Comput., **147**, pp. 547–567.

[11] Kogan, M. N., 1969, *Rarefied Gas Dynamics*, Plenum, New York.

[12] Owen, J. M. and Rogers, R. H., 1989, *Flow and heat transfer in rotating-disc systems, Vol. 1: Rotor-stator systems*, Research Studies Press, Taunton.

[13] Miklavcic, M and Wang C. Y., 2004, “The flow due to a rough rotating disk,” Z. Angew. Math. Phys., **55**, pp. 235–246.